

Durable Composites by Vulcanization of Oleyl-Esterified Lignin

Menisha S. Karunaratna,^a Charini P. Maladeniya,^a Moira K. Lauer,^a Andrew G. Tennyson,^{a,b*} and Rhett C. Smith^{a*}

^a Department of Chemistry and Center for Optical Materials Science and Engineering Technology, Clemson University, Clemson, SC 29634, USA.

^b Department of Materials Science and Engineering, Clemson University, Clemson, South Carolina, 29634, United States.

Correspondence to: Rhett C. Smith (E-mail: rhett@clemson.edu)

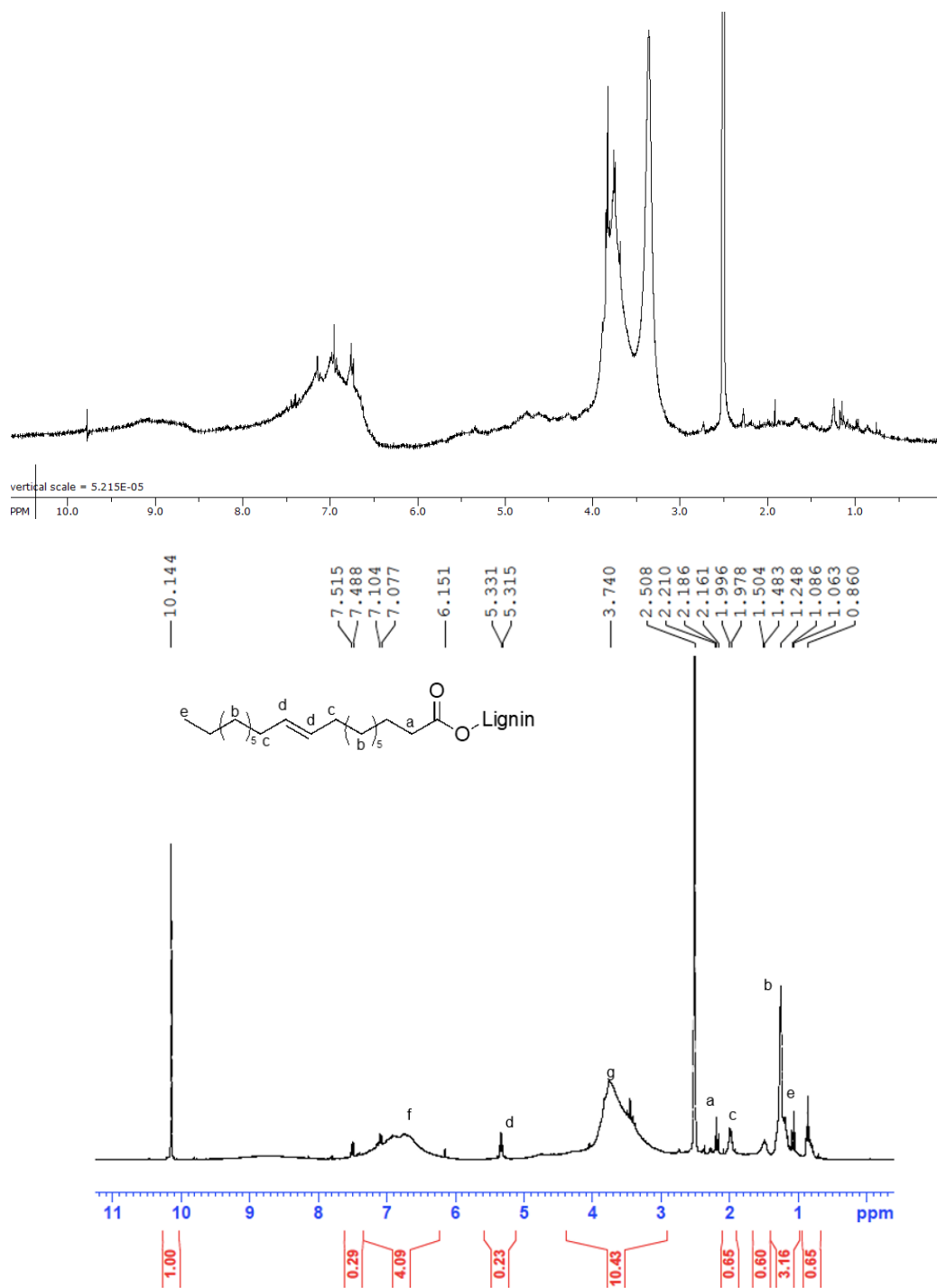


Figure S1. Proton NMR spectra for lignin starting material (upper spectrum) and of derivative EL (with 2,3,4,5,6-pentafluorobenzaldehyde added as an internal standard, lower spectrum), both in DMSO- d_6 (residual solvent signal is at 2.50 ppm). Integration of olefinic proton signal (5.3 ppm) compared to those of the 2,3,4,5,6-pentafluorobenzaldehyde internal standard (aldehydic proton resonance at 10.1 ppm) allowed calculation of olefin content per gram of EL. In addition to oleoyl-derived resonances labeled in the lower spectrum, the lignin aromatics produce peaks f and the methoxyl groups produce resonance g (the water peak in DMSO at 3.3 ppm is overlapping this region).

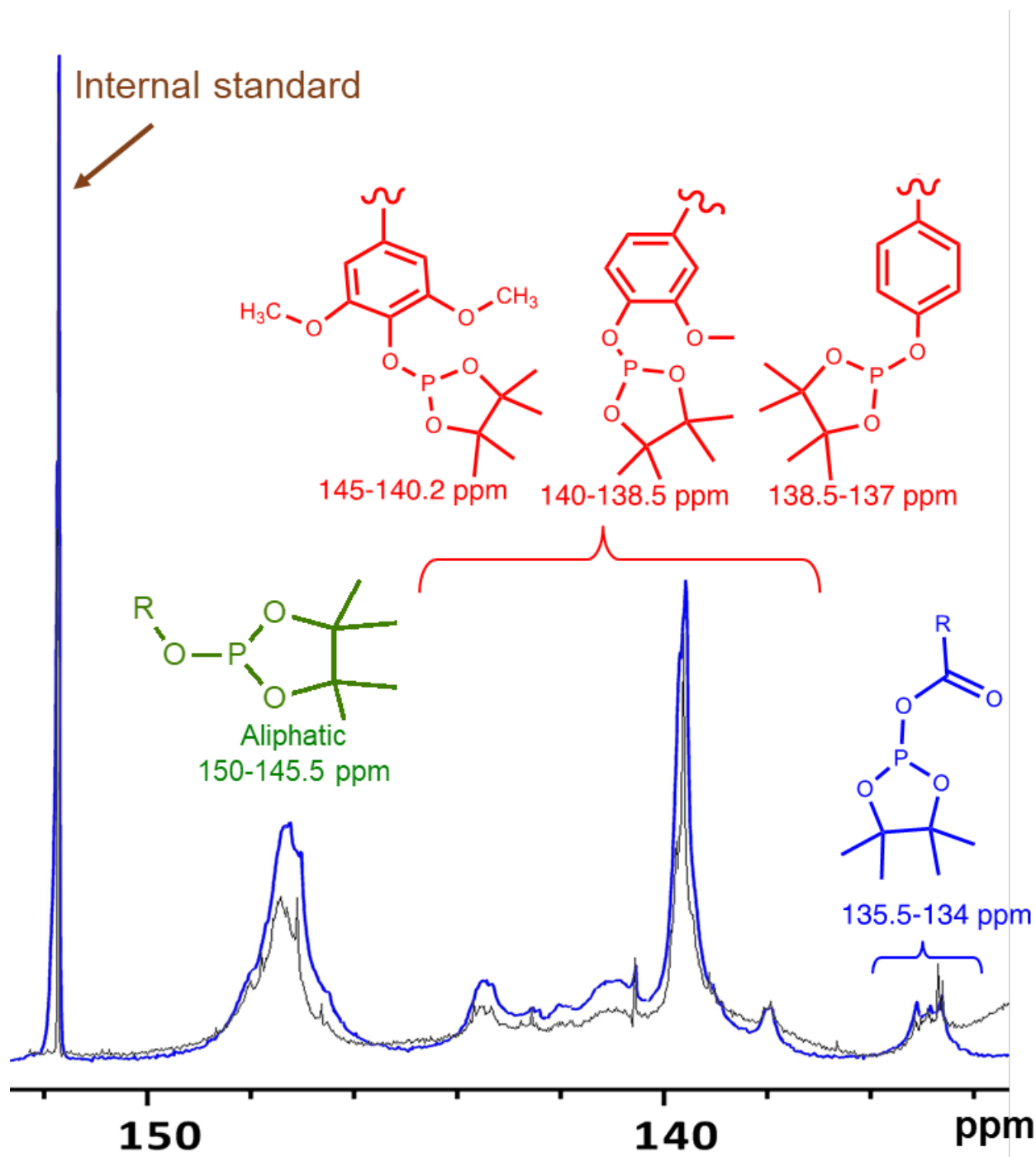
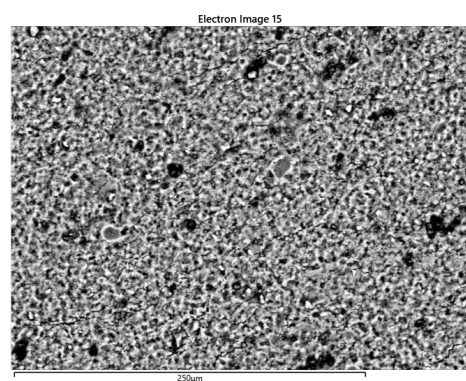
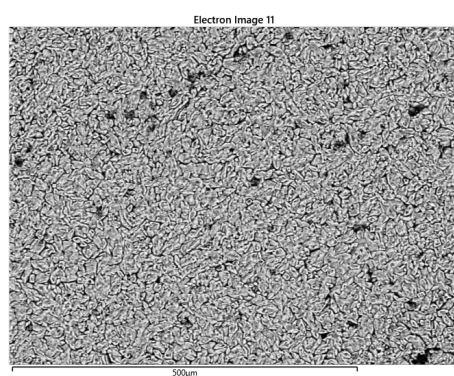
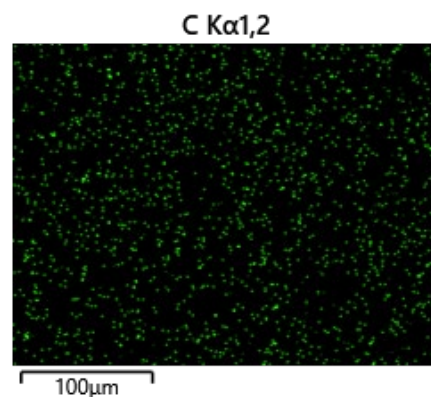
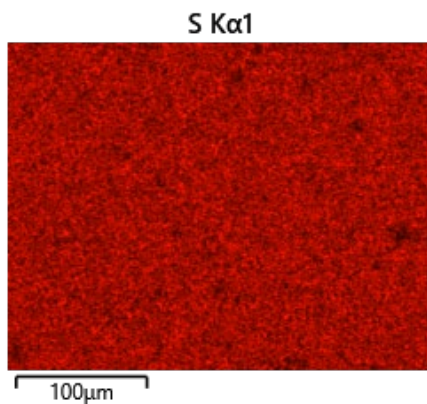


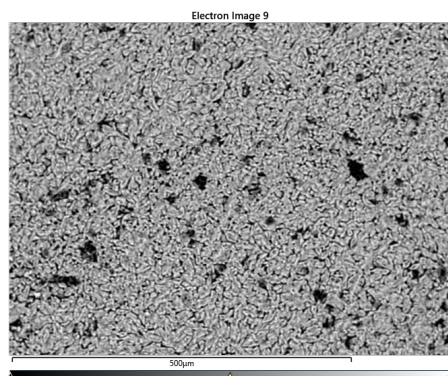
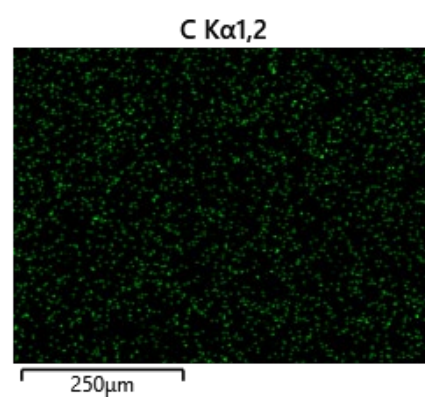
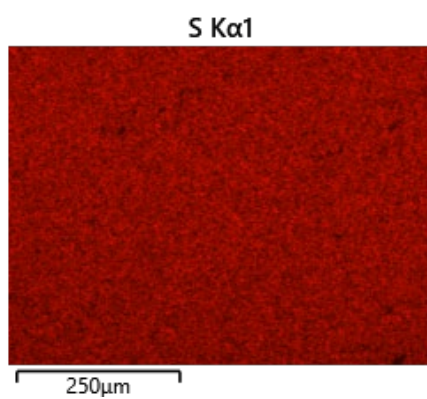
Figure S2. Phosphorus-32 NMR spectra of phosphitylated kraft lignin (generally higher-intensity blue trace) and of phosphitylated **EL** (lower-intensity black trace). For both spectra, 2-chloro-4,4,5,5-tetramethyl-1,3,2-dioxaphospholane was used as the phosphitylation agent and phosphitylated *endo-N*-hydroxy-5-norbornene-2,3-dicarboximide was used as the internal standard. Based on the integration calculation of relevant lignin subunits peaks and internal standard, the amount of total —OH present in lignin was found to be 3.5 mmol/g prior to modification and 3.2 mmol after modification.



ELS₉₀@230



ELS₉₀@180



ELS₈₀@180

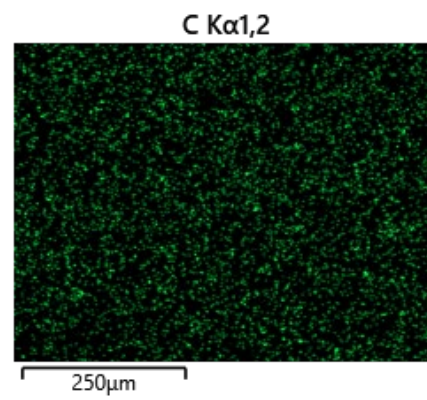
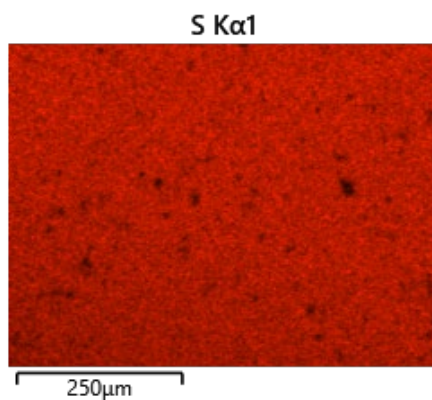
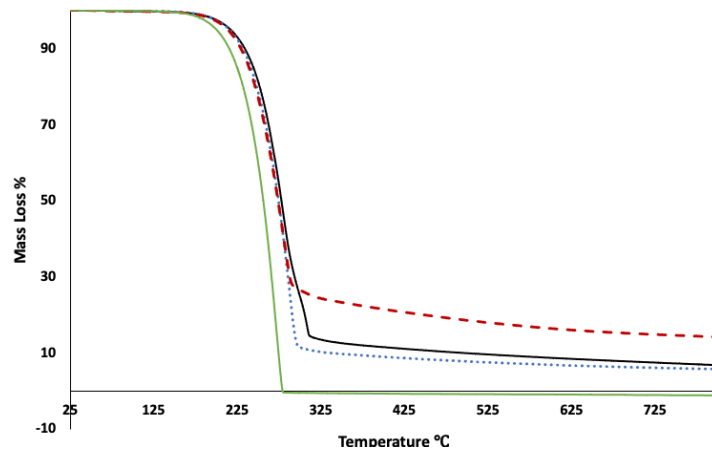
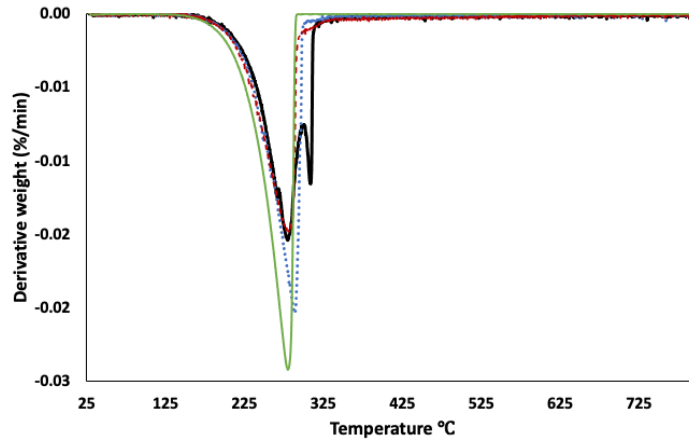


Figure S3. SEM images (left) of the prepared samples and EDX mapping (middle and right images) for sulfur and carbon. Some voids are due to deposition of a silicon oil patch during the sample preparation.

A)



B)



C)

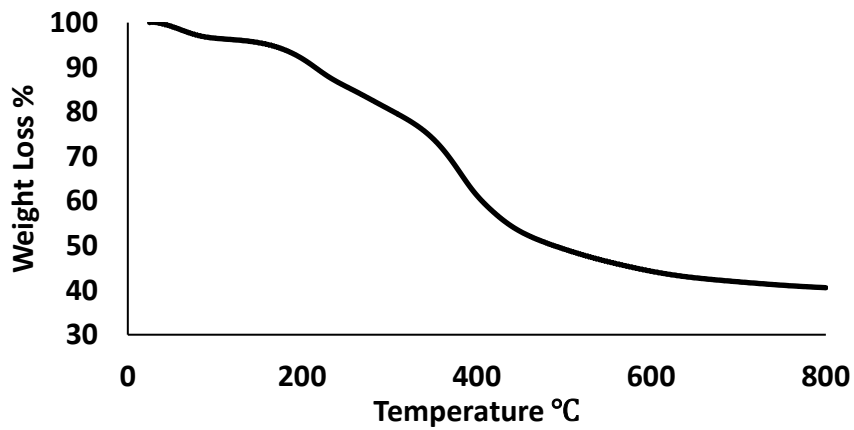
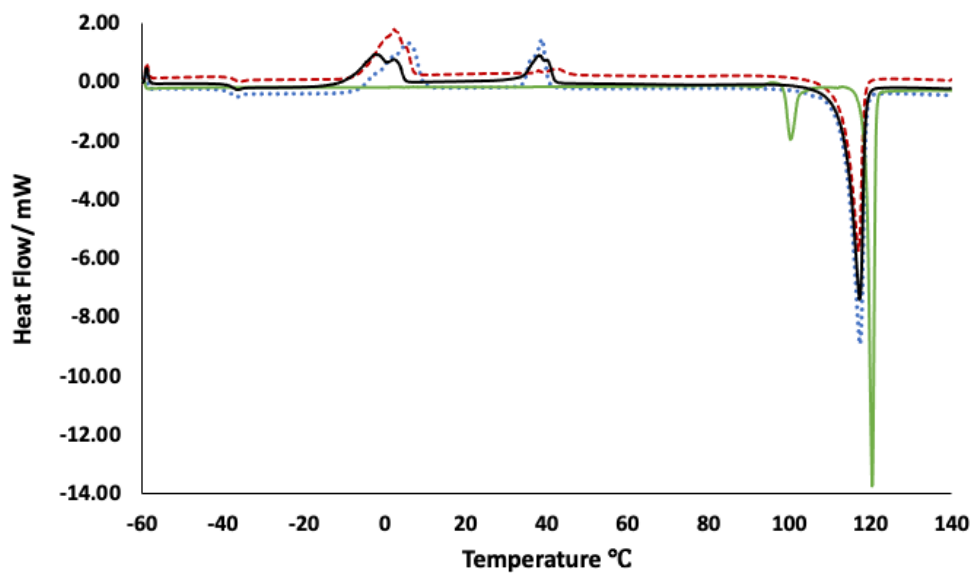


Figure S4. A) TGA curves of sulfur (green solid line), ELS₉₀@230 (black solid line), ELS₉₀@180 (blue round dotted line), ELS₈₀@180 (red square dotted line). B) DTG curves indicate the point of greatest rate of change on the mass loss curve. This clearly shows the two decomposition events of ELS₉₀@230 material. C) TGA curves of unmodified lignin.

A)



B)

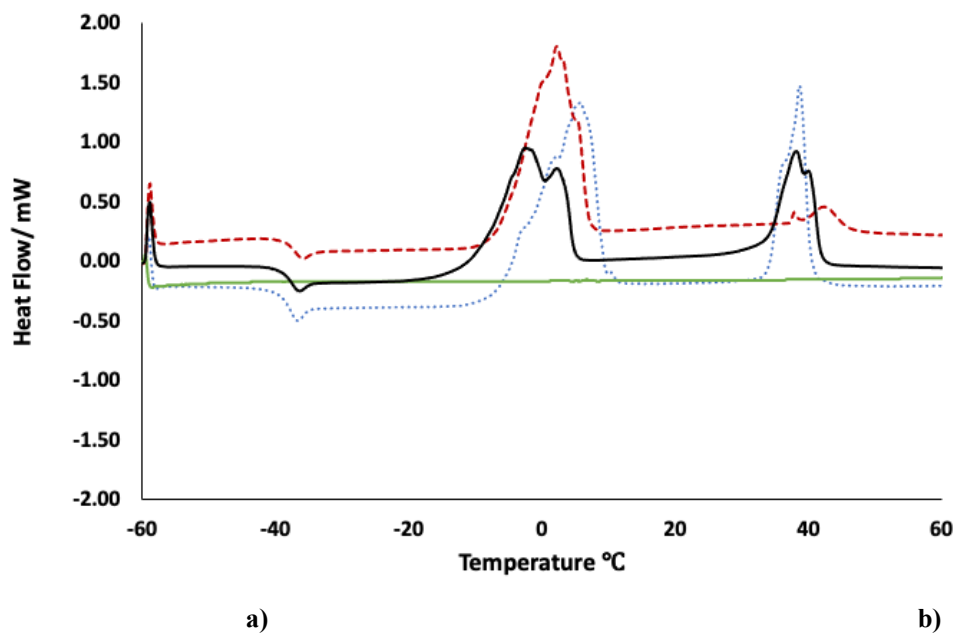


Figure S5. a) DSC curves of sulfur (green solid line), ELS₉₀@230 (black solid line), ELS₉₀@180 (blue round dotted line), ELS₈₀@180 (red square dotted line). b) The enlarged image of the DSC curves shows thermal transitions: cold crystallization peaks and glass transition temperatures.

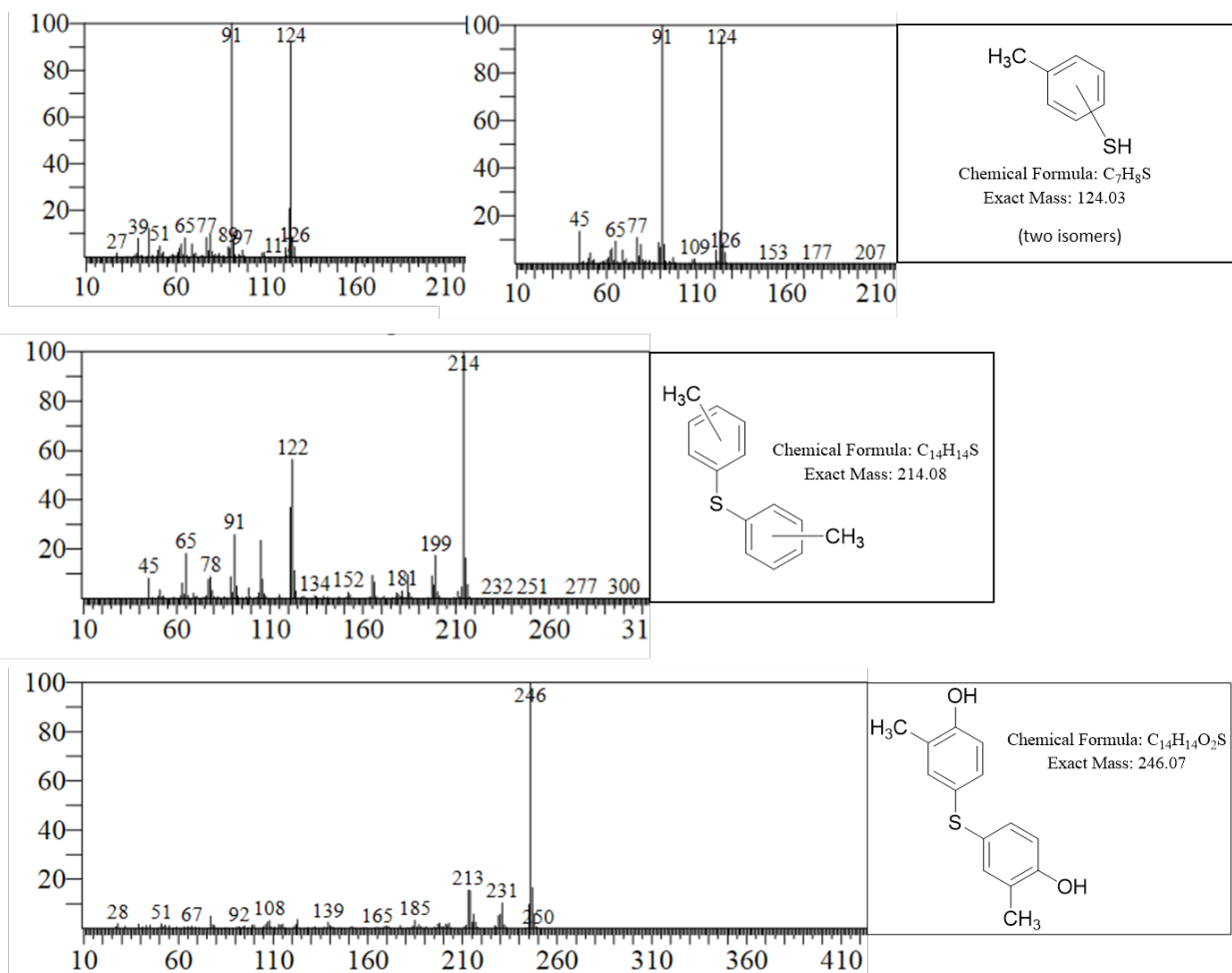


Figure S6. MS spectra confirming S-C_{aryl} bond formation to give structural subunits in EL₉₀@230 shown in Figure 3 of the manuscript.

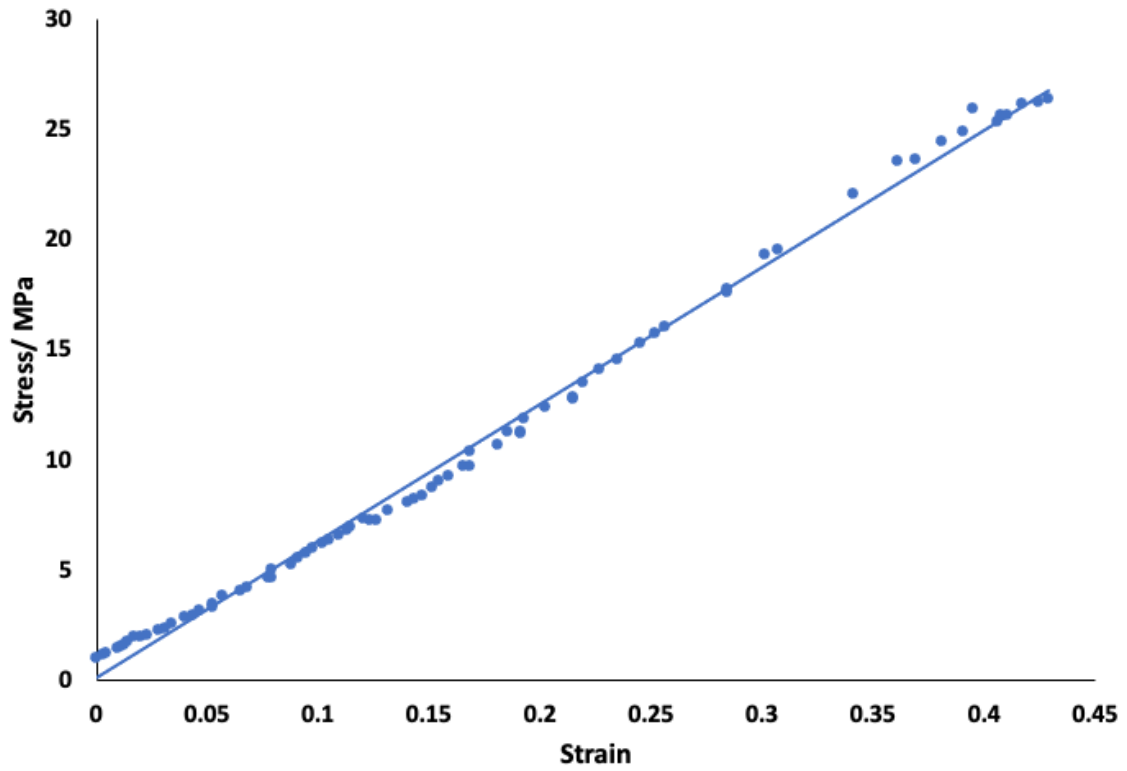


Figure S7. ELS₉₀@230 sample stress-strain graph for compressive strength analysis

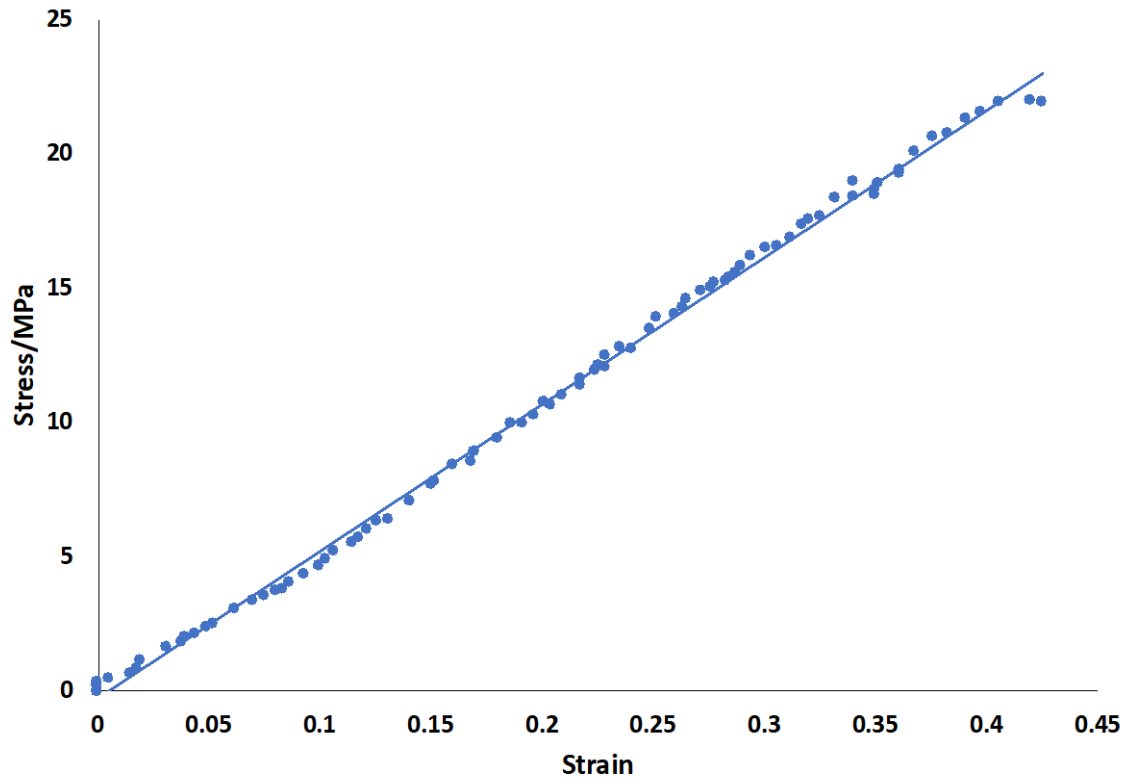


Figure S8. ELS₉₀@180 sample stress-strain graph for compressive strength analysis

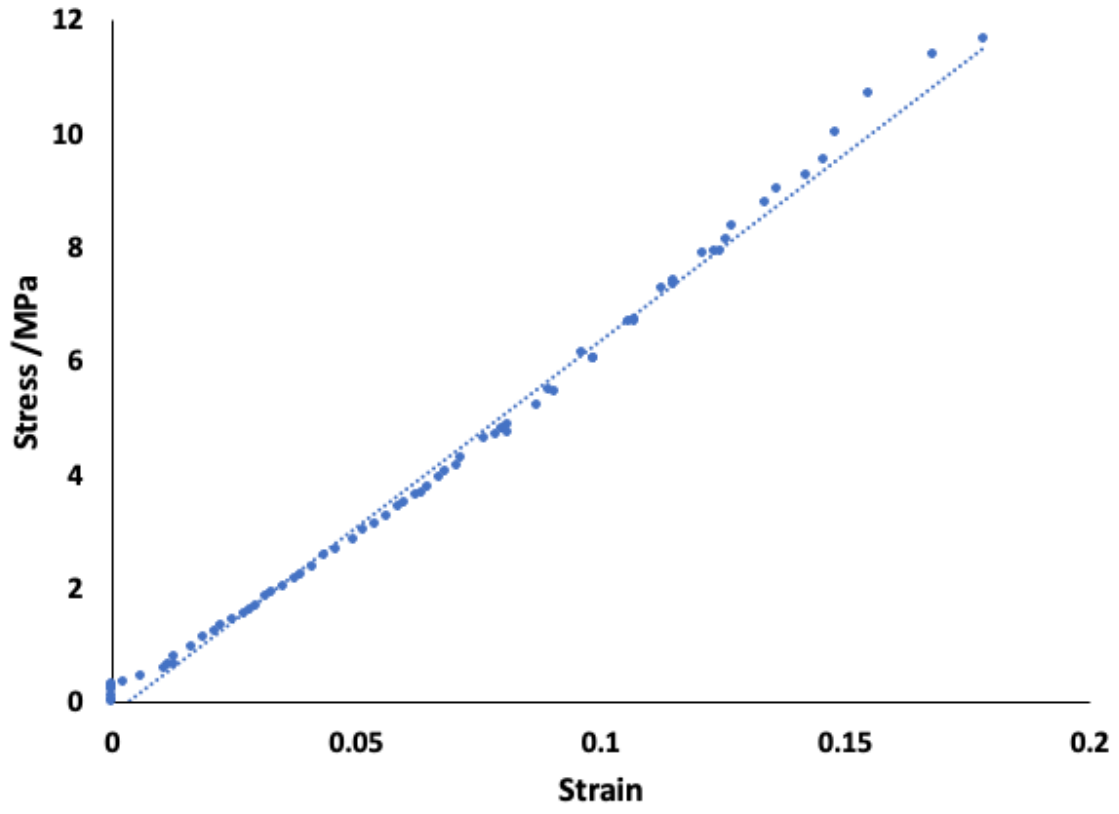


Figure S9. ELS₈₀@180 sample stress-strain graph for compressive strength analysis

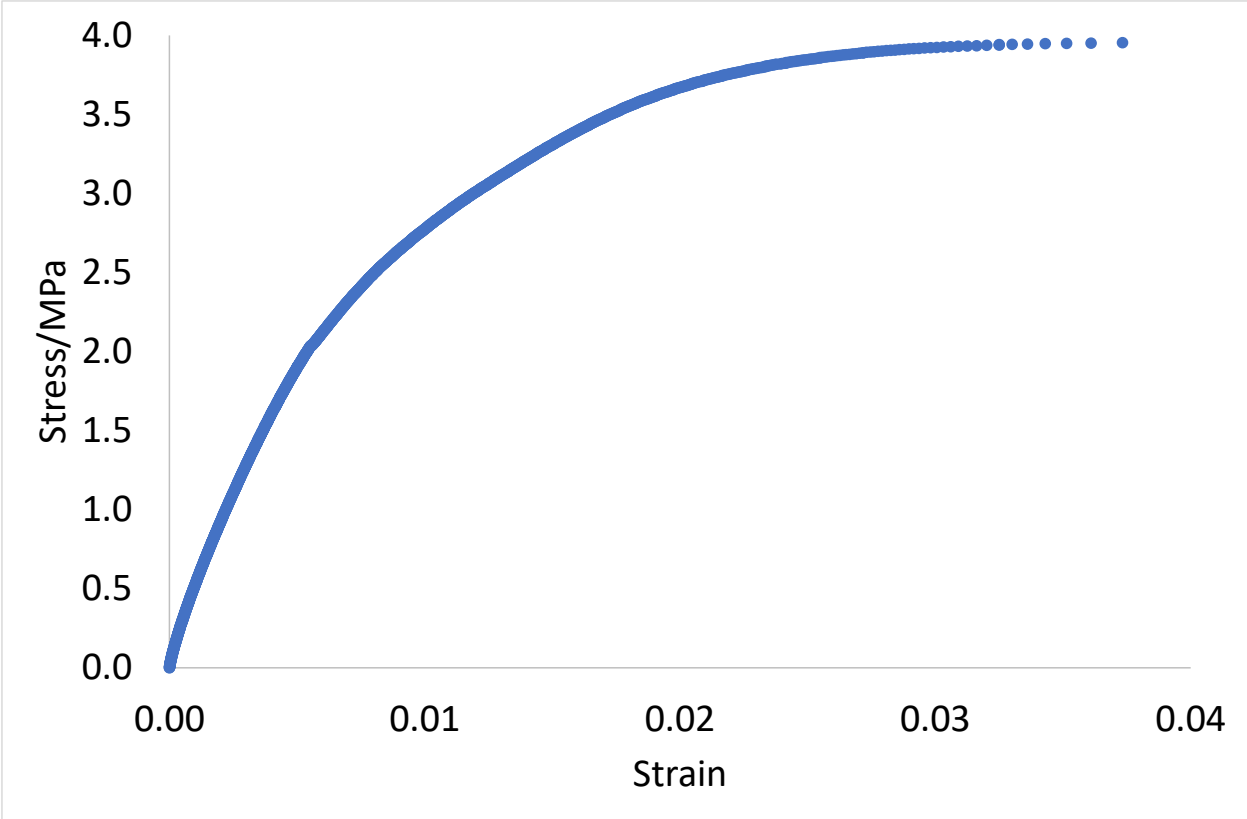


Figure S10. ELS₉₀@230 sample stress-strain graph for flexural strength analysis

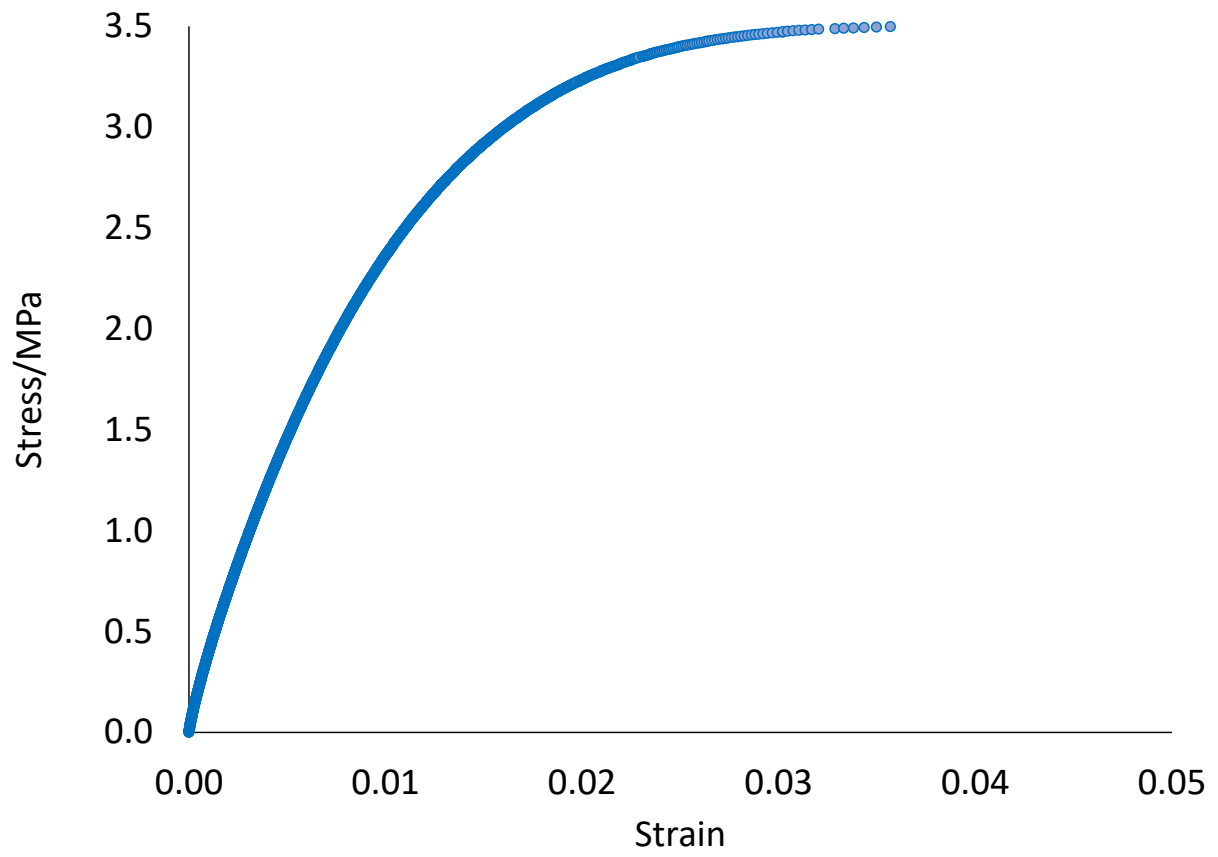


Figure S11. ELS₉₀@180 sample stress-strain graph for flexural strength analysis

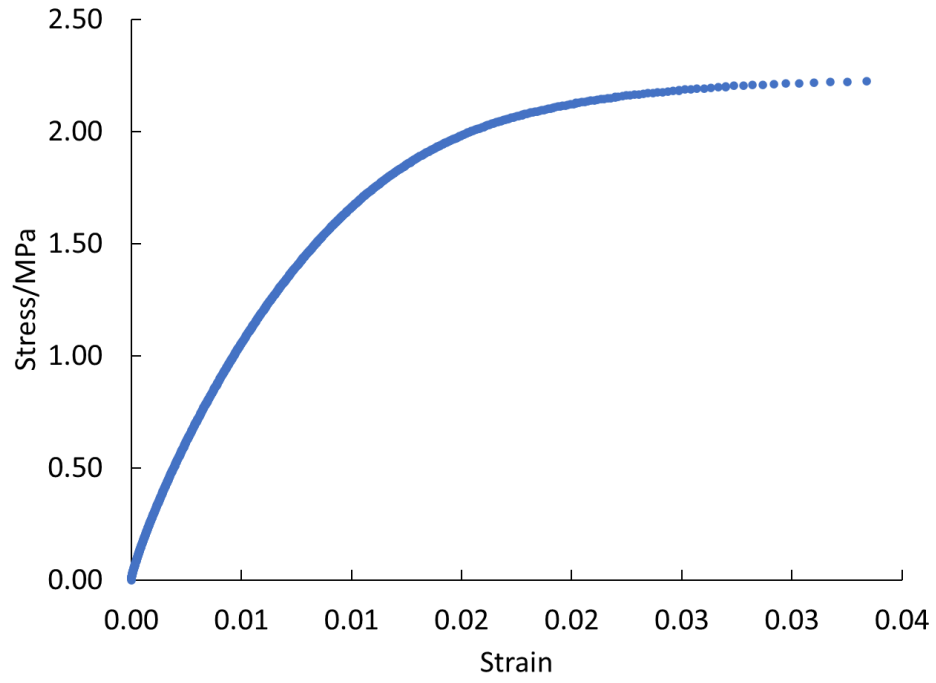


Figure S12. ELS₈₀@180 sample stress-strain graph for flexural strength analysis